molecular pharmaceutics

pubs.acs.org/molecularpharmaceutics Article

Surface Stabilization and Dissolution Rate Improvement of Amorphous Compacts with Thin Polymer Coatings: Can We Have It All?

Dunja Novakovic,* Leena Peltonen, Antti Isomäki, Sara J. Fraser-Miller, Line Hagner Nielsen, Timo Laaksonen, and Clare J. Strachan

Cite This: *Mol. Pharmaceutics* 2020, 17, 1248–1260 Read Online

ACCESS | Metrics & More | Article Recommendations | Supporting Information

ABSTRACT: The distinction between surface and bulk crystallization of amorphous pharmaceuticals, as well as the importance of surface crystallization for pharmaceutical performance, is becoming increasingly evident. An emerging strategy in stabilizing the amorphous drug form is to utilize thin coatings at the surface. While the physical stability of systems coated with pharmaceutical polymers has recently been studied, the effect on dissolution performance as a function of storage time, as a further necessary step toward the success of these formulations, has not been previously studied. Furthermore, the effect of coating thickness has not been elucidated. This study investigated the effect of these polymer-coating parameters on the interplay between amorphous surface crystallization and drug dissolution for the first time. The study utilized simple tablet-like coated dosage forms, comprising a continuous amorphous drug core and thin polymer coating (hundreds of nanometers to a micrometer thick). Monitoring included analysis of both the solid-state of the model drug (with SEM, XRD, and ATR FTIR spectroscopy) and dissolution performance (and associated morphology and solid-state changes) after different storage times. Stabilization of the amorphous form (dependent on the coating thickness) and maintenance of early-stage intrinsic dissolution rates characteristic for the unaged amorphous drug were achieved. However, dissolution in the latter stages was likely inhibited by the presence of a polymer at the surface. Overall, this study introduced a versatile coated system for studying the dissolution of thin-coated amorphous dosage forms suitable for different drugs and coating agents. It demonstrated the importance of multiple factors that need to be taken into consideration when aiming to achieve both physical stability and improved release during the shelf life of amorphous formulations.

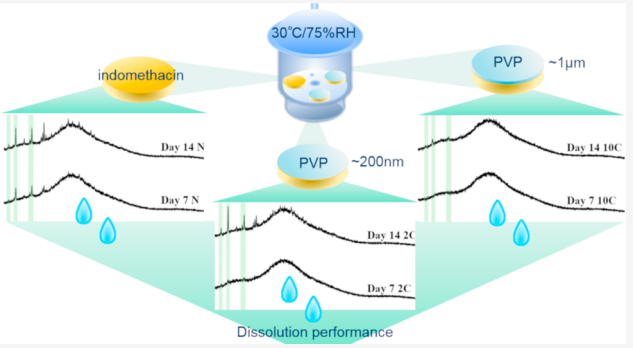

KEYWORDS: *surface crystallization, amorphous, dissolution, indomethacin, polymer coating*

1. INTRODUCTION

Surface crystallization of amorphous drugs is distinct and orders of magnitude faster than bulk (interior) crystallization.[1−6] This is believed to be due to the higher molecular mobility of surface molecules, with multiple observations in the pharmaceutical setting consistent with this theory. For instance, the crystallization of amorphous drug particles depends on their specific surface area, with smaller particles (which may otherwise be desired for improved solubility and dissolution rate), crystallizing faster and more extensively.[1,7] Further, gratings on amorphous drug surfaces flatten and disappear over time, which has been attributed to the surface molecular diffusivity being a million-fold higher than that of the bulk.[8,9] Depletion zones visualized around surface crystals are yet another example illustrating highly mobile amorphous molecular surfaces.[4,10]

The most established approach for stabilizing amorphous drugs is to form amorphous solid dispersions with polymers. While the formation of solid dispersion can stabilize the bulk, surface crystallization may still occur.[11] An approach orthogonal to amorphous solid dispersions is to stabilize the more sensitive surfaces of amorphous materials, with or without additionally stabilizing the bulk of the material. This strategy benefits from a lowered polymer (or other excipient used for stabilization) burden and ideally should be simple and scalable. Whether or not this approach requires specific types of interactions between the drug and the stabilizing agent or

Received: December 12, 2019
Revised: February 5, 2020
Accepted: February 6, 2020
Published: February 6, 2020

https://dx.doi.org/10.1021/acs.molpharmaceut.9b01263
Mol. Pharmaceutics 2020, 17, 1248−1260

whether the principle of physical coverage on its own is enough to lower the molecular mobility at the surface to that of the bulk is still uncertain.

In 2006, Wu and Yu demonstrated that simple amorphous drug film surface coverage with a microscope slide (silicate coverslip) inhibited crystallization, and this can broadly be considered the initial pharmaceutical research into surface crystallization.[1] Subsequently, gold and strong polymer polyelectrolytes were among the first materials shown to inhibit the surface crystallization of amorphous drugs in coating layers as thin as 10 and 3−20 nm, respectively.[3,12] Surface stabilization by the pharmaceutically more relevant dextran, alginate, and chitosan followed, among other studies. While the gold film was sputtered or vacuum deposited,[3] the strong polymer polyelectrolyte[12] and dextran,[5] alginate,[6] and chitosan[13] films were selected and deposited based on the coating material having a charge opposite to that of the drug molecule, resulting in ionic interactions between the drug and the coating. Thin polymer coatings have also been used to stabilize solid dispersions, with the same polymer used as both the matrix and coating agent.[14] Dry coating of solid dispersions with carnauba wax also resulted in a very stable product, where the matrix was stabilized with a different polymer.[15] More recently, 20 nm thick gelatin efficiently inhibited surface crystallization with no strict requirement of opposite charges between the drug and the stabilizing agent.[16]

While these studies highlight the potential of diverse coatings to inhibit surface crystallization, surface coating studies involving polymers used as pharmaceutical excipients are limited.[5,6,13,16,17] The majority of these surface coating studies have focused on the improvement of storage stability of amorphous systems. Additionally, some of the study designs are not likely to be implemented on a larger scale due to pharmaceutically irrelevant materials or difficult-to-scale processes, involving multiple steps (preparation of amorphous material, preparation, and consequent coating and rinsing/drying of particles, from which the final dosage form must be made). Furthermore, the dissolution performance as ultimately the most important critical quality attribute of such systems remains less studied,[5,6,13] particularly, in stability monitoring.[12] Studies thus far have focused on the dissolution of individually coated amorphous particles[5,6,13] or such particles compressed into a tablet.[12] As the ultimate goal of amorphous drug formulations is to improve solubility and oral bioavailability, the stabilized amorphous drug systems must perform well in dissolution testing during the full shelf life, in addition to having adequate physical stability.

This study investigates the surface stabilization of a simple dosage form consisting of an amorphous drug compact that was subsequently spray-coated with a thin polymer layer. As only the final amorphous dosage form (compact) is coated instead of individual drug particles, the total amount of polymer used is minimized. We wanted to see if such a simple system with this minimal amount of a coating agent can provide maintenance of the intrinsic dissolution rate during dissolution in a pharmaceutically relevant setting. In addition, the effect of coating thickness (a varying amount of polymer coating) on the interplay between stabilization during storage and dissolution was investigated.

2. MATERIALS AND METHODS

2.1. Sample Preparation. *2.1.1. Preparation of Different Solid-State Forms of Indomethacin.* Amorphous indomethacin was prepared by melting the γ form (Hovione FarmaCiencia SA, Loures, Portugal) at 170 °C, followed by cooling to 5 °C. The α form of indomethacin was prepared by adding Milli-Q water to an ethanol solution of indomethacin at 80 °C. Precipitated crystals were vacuum filtered and dried overnight. The ε form of indomethacin was prepared from the slurry of an amorphous form in pH 6.8 buffer.[18,19] The solid-state forms were confirmed with X-ray diffractometry (XRD), attenuated total reflectance Fourier transform infrared spectroscopy (ATR FTIR), and differential scanning calorimetry (DSC).

2.1.2. Preparation of Compacts with Vacuum Compression Molding. Amorphous indomethacin was loaded into a polytetrafluoroethylene (PTFE) Teflon foil lining within the MeltPrep cylindrical chamber (MeltPrep GmbH, Graz, Austria). Compacts were formed by vacuum compression molding (VCM)[20,21] at 70 °C (above the T_g of indomethacin) for 10 min, followed by cooling for 10 min on a steel unit. This corresponds to an approximate cooling rate of 5 °C per minute. The piston (20 mm in diameter) created a compaction pressure of 2.6 bar. The resulting compacts were transparent, yellow, and brittle, much like the solidified melt upon quench cooling. The compacts weighed 500 ± 10 mg and had a height of approximately 1.3 mm and a diameter of 20 mm. Their amorphous nature was confirmed with polarized light microscopy (PLM) through an absence of any visible birefringence, and XRD, by the presence of an amorphous halo. These compacts are referred to as uncoated (N) throughout the study.

2.1.3. Preparation of Compacts with Hydraulic Compression. Compacts composed of α indomethacin were prepared by manual hydraulic compression (Manual Hydraulic Press, Specac Ltd., Orpington, U.K.) for 30 s with 1 ton and were further used as a reference for intrinsic dissolution testing.

2.1.4. Ultrasonic Spray Coating of Compacts. Some of the freshly prepared amorphous indomethacin compacts were spray-coated with polyvinylpyrrolidone (PVP K30, average molecular weight (M_w) 40 000, Sigma-Aldrich, St. Louis, Missouri, USA) using an Exacta Coat Ultrasonic Spraying system (Sonotec, Milton, New York, USA). Prior to coating, the samples were kept in a desiccator with silica pearls. The coating solution was 0.5% w/v PVP K30 in Milli-Q water.[22] Compacts were placed on a temperature-controlled sample stage and sprayed with a polymer solution from the ultrasonic spraying nozzle placed above the compact. One of the compact faces was coated by programing the path of the nozzle in the x and y directions, while keeping the distance of the nozzle from the samples (z) the same.[22] The number of coating cycles (full paths of the nozzle above the sample) applied was either two (2C) or ten (10C), resulting in coatings hundreds of nanometers or approximately a micrometer in thickness, respectively. The coating solution was applied at an infusion rate of 0.1 mL/min. Taking into account the coating and dwell times, as well as the starting concentration of PVP solution, it can be estimated that 10 cycles of coating corresponded to a deposition of a maximum of 4.45 mg of PVP per compact, which weighed 500 mg (roughly 1% w/w). To ensure complete coalescence of the sprayed droplets, the sample stage below the nozzle was heated to 30 °C (below the T_g of indomethacin), with a dwell time of 30 s in between each coating cycle. PVP was selected as a stabilizing agent due to its documented ability to stabilize amorphous indomethacin.[23,24]

2.1.5. Storage. The stability of the compacts was monitored during storage at 30 °C and 75% relative humidity (RH),

https://dx.doi.org/10.1021/acs.molpharmaceut.9b01263
Mol. Pharmaceutics 2020, 17, 1248−1260

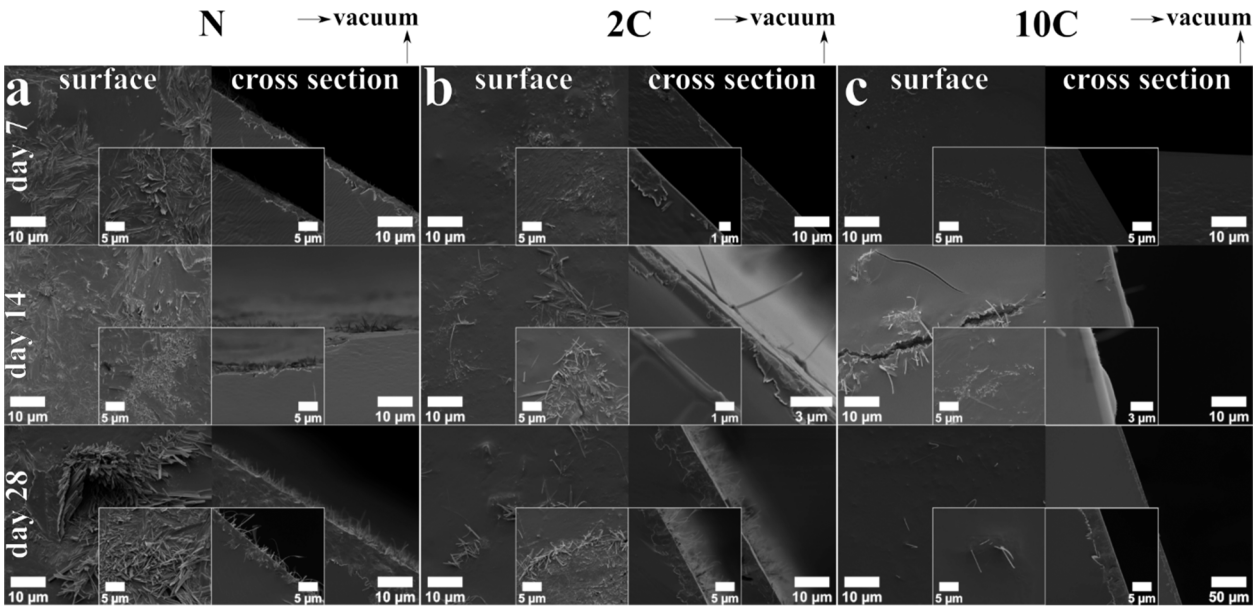

Figure 1. SEM micrographs of the top surface and cross sections of amorphous indomethacin compacts stored at 30 °C/75% RH; (a) uncoated (N), (b) PVP-coated with two spraying cycles (2C), and (c) PVP-coated with ten spraying cycles (10C). The black areas on the top right of some cross-sectional images represent a vacuum. This is also indicated by arrows in the figure.

obtained with a saturated solution of sodium chloride. Day 0 uncoated samples were analyzed within 24 h of preparation. All coated samples had their polymer-coated side exposed to the humid environment.

2.2. Analytical Methods. *2.2.1. Scanning Electron Microscopy (SEM).* For imaging the compact faces, compact sections were placed on stubs covered with double-sided carbon tape. To image compact cross sections, compacts were broken to create new surfaces perpendicular to the top surface just before platinum sputter coating. The micrographs were collected with an FEI Quanta 250 field emission gun SEM (FEI, Hillsboro, USA) microscope using a high vacuum, a voltage of 3−5 kV, and an Everhart Thornley Detector (ETD).

2.2.2. X-ray Diffractometry (XRD). Diffractograms were obtained using a Malvern Panalytical Empyrian (PANalytical B.V. Almelo, The Netherlands) instrument in reflection mode with Cu $K\alpha_1$ radiation (λ = 1.5406), divergence slit of 0.19 mm, generator voltage of 45 kV, and a tube current of 40 mA. Diffractograms were collected from 5 to 50° 2θ with a step size of 0.013°. The compacts were rotated during the measurements.

2.2.3. Attenuated Total Reflectance Fourier Transform Infrared Spectroscopy (ATR FTIR). A minimum of triplicate infrared spectra of the compact faces was obtained using a Vertex 70 spectrometer (Bruker Optics, Ettlingen, Germany) equipped with a MIRacle ATR single-reflection crystal (Pike Technologies, Wisconsin, USA) and a DLaTGS detector. The spectra (averages of 256 scans with a spectral resolution of 4 cm^{-1}) were collected using OPUS 8.1 (Bruker Optics, Ettlingen, Germany) software.

2.3. Intrinsic Dissolution Testing. Dissolution tests were performed using the Erweka DT6 paddle apparatus (Erweka GmbH Langen, Germany) operated at 50 rpm. Prior to the dissolution experiments, the radial band and one round flat surface of each of the compacts were coated with transparent nail polish containing nitrocellulose and tosylamide/epoxy resin (shellac) as waterproof agents (Mavala Switzerland base coat).[12] In this way, only one surface of the compacts was exposed to the dissolution medium, allowing intrinsic dissolution testing analysis. Where applicable, the exposed surface was that previously coated with the PVP. Compacts (obtained by vacuum compression molding) had an exposed face surface area of 3.14 cm^2, while the reference tablets composed of α indomethacin (prepared by hydraulic single punch press) had a corresponding area of 1.33 cm^2. The dissolution medium was 900 mL of phosphate buffer with a pH of 6.8 at 37 °C. Dissolution medium samples were withdrawn at selected time points and replaced with the same volume of preheated buffer. The dissolved drug concentration (unfiltered samples) was measured with UV spectrophotometry (UV-1600PC UV−Vis spectrophotometer, VWR, China) at 318 nm. All dissolution experiments were performed in triplicate. The compacts remained as one piece after 45 min of dissolution testing, which allowed for their collection from the dissolution vessel and subsequent solid-state analysis.

3. RESULTS

3.1. Coating Thickness and Uniformity. Coating thickness and uniformity, as well as the adherence to the compacts, were assessed based on SEM images of compact surfaces and cross sections. As can be seen from cross-sectional SEM images in Figure 1, the core of the tablet and coating layers exhibited different appearances and allowed for estimation of the coating thickness: 10 coating cycles produced final coatings roughly 1 μm thick, whereas 2 coating cycles formed a layer approximately 200 nm thick. The coating appeared uniform and well adhered to the surface of the drug compacts throughout the storage study. For instance, the surface of samples coated with 10 cycles on day 7 revealed a smooth coating that was still intact, while the cross-sectional images suggested complete adherence.

3.2. Effect of Coatings on Physical Stability during Storage. *3.2.1. Morphological Analysis.* The stability of the uncoated (N) samples was compared to the two types of PVP-coated samples (coated with two (2C) or ten (10C) spraying cycles) by monitoring for up to 28 days of storage at 30 °C/

https://dx.doi.org/10.1021/acs.molpharmaceut.9b01263
Mol. Pharmaceutics 2020, 17, 1248−1260

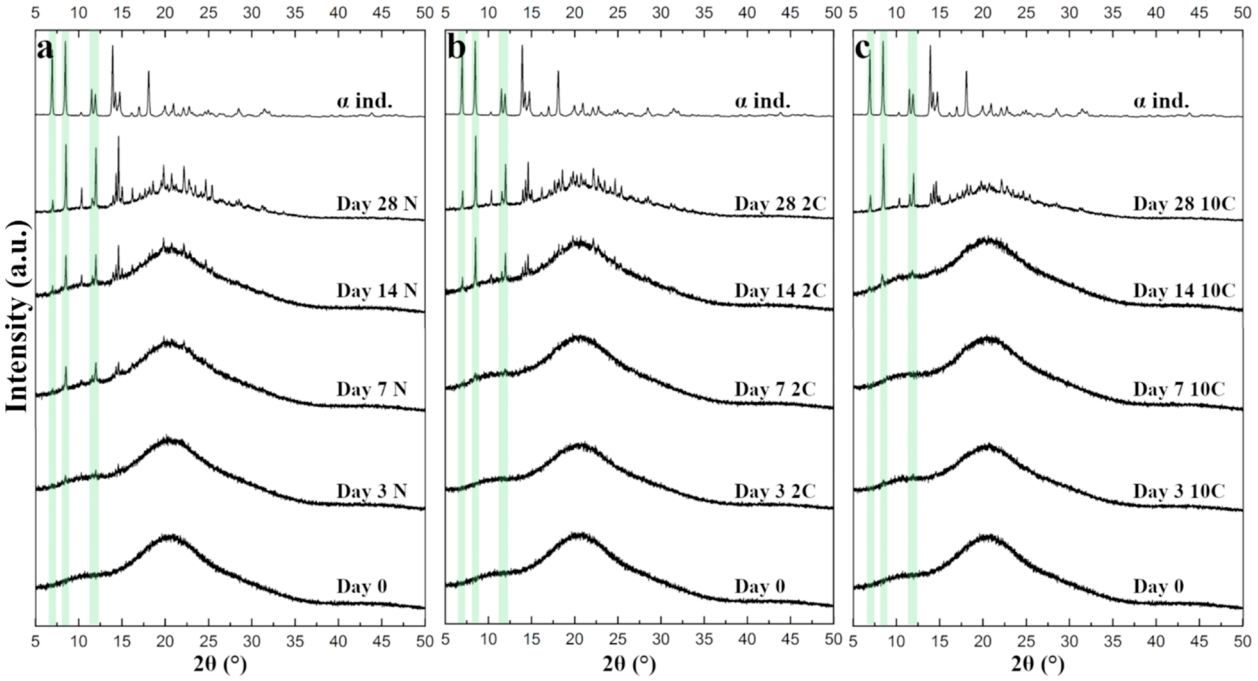

Figure 2. XRD reflection patterns of (a) uncoated (N), (b) PVP-coated with two cycles (2C), and (c) PVP-coated with ten cycles (10C) amorphous indomethacin compacts during storage at 30 °C/75%RH. In all cases, day 0 represents the neat amorphous (uncoated) indomethacin compact within 24 h from preparation. Characteristic peaks of α indomethacin are marked in green.

75% RH. As both coated and uncoated samples were prepared in the same manner with VCM, any potential nucleation sites (undetected with PLM and XRD) would have been similarly present in all studied samples, which allowed for direct comparison of their crystallization tendency. First, we wanted to see whether the crystallization was surface biased qualitatively. Crystallization progression was estimated based on the SEM micrographs of the compact surfaces and cross sections. Surface and cross sections of the day 0 sample exhibited a smooth appearance (Figure S1). Figure 1 provides an overview of differences among the samples stored for 7, 14, and 28 days. In all samples, the crystallization was limited to a thin layer at the compact drug surface, no deeper than 50 μm on the 1.3 mm thick compacts, despite the moisture acting as a plasticizer, which, if absorbed beyond the surface into the core, would theoretically promote crystallization in the core as well.[25] This is easily seen, especially in the cross-sectional SEM images, as both the amorphous drug and polymer appear smooth, in contrast to the roughly textured crystalline areas. All observed crystals were needle-shaped.

The crystallization during storage included growth both out of and into the interior of the compacts. The cross-sectional images revealed that the surface crystallization first progressed toward the interior of compacts, with crystals sporadically emerging above the surface after 7 days, mostly on the uncoated samples. The surface view of the same samples revealed that, at that time point, the crystals were largely aligned with the surface, while at 14 or 28 days, the crystals grew in number and protruded up to 5−10 μm above the compact surface. With both the 2C- and 10C-coated samples, the needle crystals appeared to grow from underneath the coating and then emerge above the coated surface. For instance, images of the 2C samples at day 7 reveal that some of the needles penetrated through the coating, while others were still covered by the polymer.

SEM images indicate that the coating presence, as well as thickness, influenced crystallization behavior in both the outward and inward directions. This is particularly evident at the end of the storage study. Almost the entire surface of the day 28 N samples was covered with needle-shaped crystals proceeding both outward and inward. In comparison, coated samples had fewer areas with outward growing crystals. The density of these areas was higher with the thinner coating; the thicker coated surface was still mostly devoid of crystals. In addition, the cross-sectional images show that the crystallization toward the interior was slightly deeper for the thinner coating and was similar to the uncoated samples. Depletion zones in between amorphous and crystalline areas were also visible, particularly in the early days of storage with the uncoated samples. For instance, the top surface of the uncoated sample on day 3 depicts such zones, which resemble microcracks (Figure S2).

3.2.2. Solid-State Analysis. XRD and ATR FTIR were employed for complementary solid-state characterization. As the compacts were rotated during the XRD measurements and the scans were performed in reflection, the diffractograms depicted in Figure 2 show the average solid-state profile biased toward the compact surfaces. Taking into account the density of discs and the element weight fractions of indomethacin, it can be estimated that 90% of the diffraction signal originates from within 200 μm of the surface, whereas 50% of the diffraction is generated from within 100 μm of the surface (Figure S3). On the other hand, ATR FTIR measurements shown in Figure 3 provide even more surface-specific solid-state information, with sampling from a minimum of three different regions at the sample surfaces. Based on refractive indices of PVP and diamond (approximately 1.5 and 2.4, respectively) and an angle of incidence of 45°, it can be estimated that the depth of penetration of the evanescent wave in this set up was between 1.34 and 1.01 μm in the spectral

https://dx.doi.org/10.1021/acs.molpharmaceut.9b01263
Mol. Pharmaceutics 2020, 17, 1248−1260

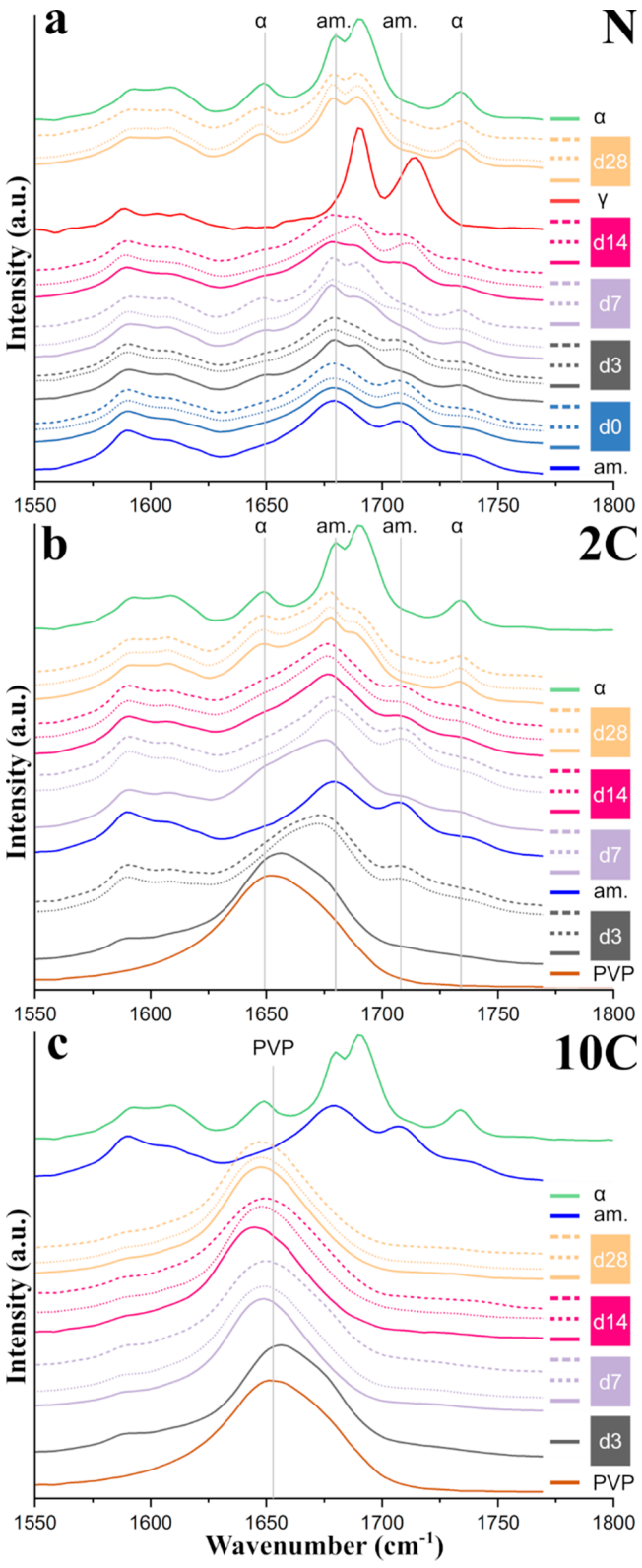

Figure 3. ATR FTIR spectra of (a) uncoated (N), (b) PVP-coated with two cycles (2C), and (c) PVP-coated with ten cycles (10C) amorphous indomethacin compacts during storage at 30 °C/75%RH; am = amorphous.

range of 1500−2000 cm^{-1}. In addition to the more global (XRD) versus targeted area and surface-biased (ATR FTIR) sampling, the selected characterization techniques are especially complementary, as ATR FTIR is highly sensitive to the presence of PVP, which, being amorphous, can be considered invisible to XRD in this context.

As can be seen in Figures 2 and 3, the PVP coating delays the onset of crystallization at 30 °C/75% RH. According to the XRD analyses (Figure 2), the first signs of crystallization were observed at day 3 for uncoated samples, day 7 for 2C-coated samples, and day 14 for 10C-coated samples. The onset of crystallization estimated with the XRD matches the ATR FTIR results (Figure 3), with the exception of the 10C-coated samples, whose PVP coating layer dominated the ATR signal. As mentioned above, the depth probed with ATR FTIR in the wavenumber region of interest in the current study is estimated to be just above 1 μm, which explains why the PVP signal (of ~1 μm thick layer) dominated the spectra of 10C-coated samples.

Another interesting observation from the ATR FTIR spectra (Figure 3c) is a trend of the PVP carbonyl stretch peak to shift toward lower wavenumbers during storage, which is likely due to polymer−water interactions.

As expected from previous studies,[26,27] crystallization of the amorphous indomethacin at 75% relative humidity was predominantly to the α form. Exceptionally, one ATR FTIR spectrum of the uncoated sample on day 14 was dominated by the signal from the γ form. With a sampling area of 2.5 mm^2, this demonstrates some degree of heterogeneity in the resulting polymorphs, as has been observed previously.[27] Overall, these results indicate that crystallization inhibition depends on the coating thickness, a thicker coating provided protection for a longer period of time.

3.3. Effect of Coatings on Dissolution Performance.

3.3.1. Dissolution Behavior. The intrinsic dissolution behavior of uncoated versus polymer-coated samples with two different coating thicknesses was tested for 45 min in pH 6.8 phosphate buffer. The reported solubility of indomethacin at this pH is 835 μg/mL,[28] which greatly exceeds the highest measured concentrations, confirming that the sink conditions were maintained in this study. Cumulative dissolved amounts of drug versus time profiles are depicted in Figure 4. Intrinsic dissolution rates (IDR) were calculated by linear regression from the early time points. Improvement in IDR of the amorphous versus α form of indomethacin was approximately 2-fold in the first 10 min of the tests.

During the initial stages of dissolution, lasting for approximately 5 min, we can assume that no significant solution-mediated crystallization is taking place, as the profiles appear linear. During this initial phase of dissolution, there was a trend toward a decreased dissolution rate upon increased storage time for the uncoated samples, with day 28 samples having the lowest IDR (Figure 4a). During this same time period, the dissolution profiles for both 2C- and 10C-coated samples closely follow that of the fresh uncoated amorphous samples (day 0), even upon being subjected to a short storage time at high humidity (Figure 4b,c). In contrast, the coated samples stored for longer periods of time trended toward a decreased IDR when compared to the fresh uncoated amorphous samples. This can be best seen from Figure 4b, where the dissolution profiles of the day 3 and day 7 samples closely resemble that of the fresh uncoated amorphous samples, whereas the day 14 and day 28 samples are rather similar to the profile of α indomethacin. Similarly, the IDR of the 10C-coated samples stored for 14 days was also equal to that of the uncoated amorphous indomethacin, however, for a shorter duration of dissolution, when compared to the 2C

https://dx.doi.org/10.1021/acs.molpharmaceut.9b01263
Mol. Pharmaceutics 2020, 17, 1248−1260

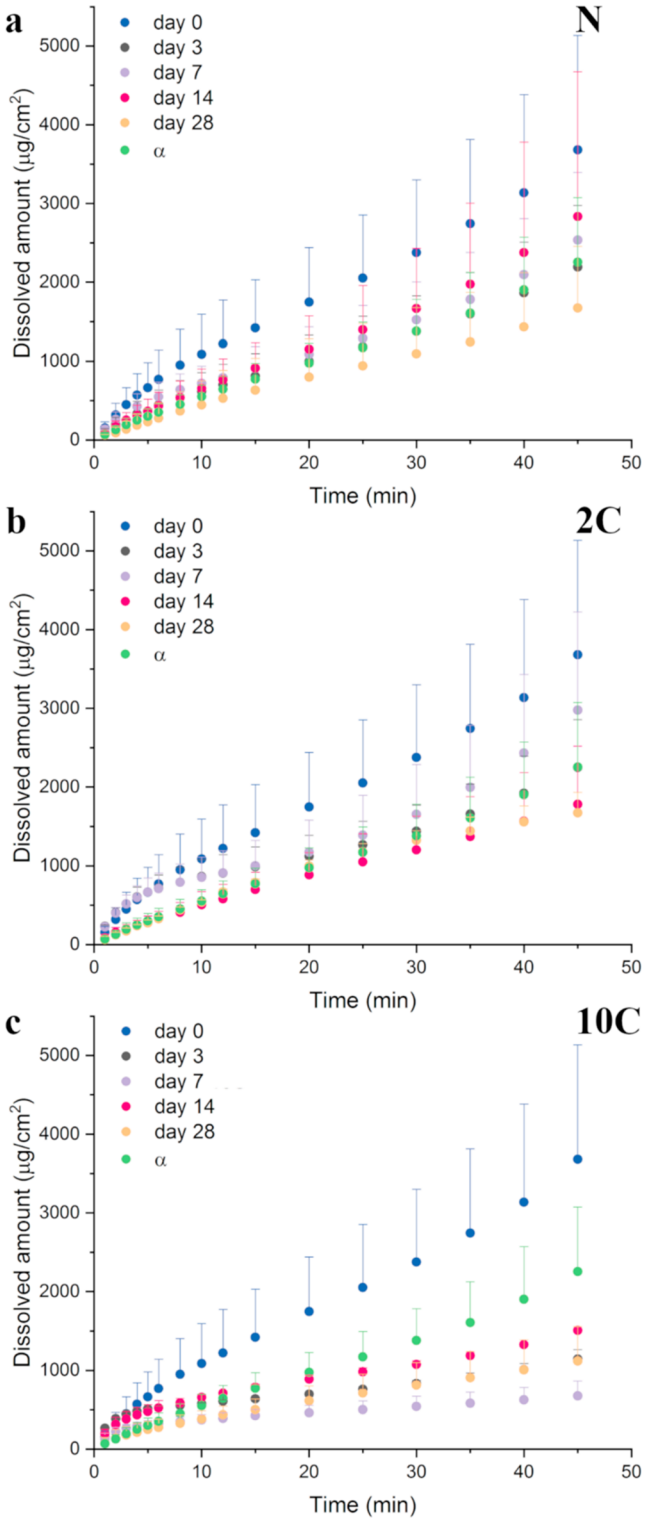

Figure 4. Intrinsic dissolution profiles of (a) uncoated (N), (b) PVP-coated with two cycles (2C), and (c) PVP-coated with ten cycles (10C) amorphous indomethacin compacts during storage at 30 °C/75%RH. Profiles represent mean values plus one standard deviation of three measurements. The α indomethacin is uncoated in all graphs.

samples. This correlates well with the overall preserved amorphous nature of coated samples stored short-term prior to dissolution (Figures 2 and 3); up to day 7 for the thinner coatings and up to day 14 for the thicker coatings.

In the second phase of dissolution, during which curvature in the dissolution profiles (which typically indicates a solution-induced crystallization) was observed, there is a clear difference between the uncoated and 2C-coated samples on the one hand and the 10C-coated samples on the other hand. This is evident when the profiles are compared to that of the uncoated α indomethacin tablets (color-coded in green in Figure 4). Whereas the uncoated and 2C-coated samples are distributed around the α indomethacin profile, all 10C-coated samples have profiles whose concentrations were below those of the α indomethacin. Thus, the dissolution behavior was dependent on the original coating thickness.

3.3.2. Surface Morphology upon Dissolution. A comparison of surfaces and cross sections of compacts after 45 min of dissolution testing is depicted in Figure 5. In general, the surface of uncoated samples was much rougher after the dissolution testing. On the other hand, the surface of the coated samples, especially with 10C, was still smooth in many areas even after dissolution testing. For instance, after 28 days of storage, both the 2C- and 10C-coated samples contained smooth amorphous looking regions among the crystallized zones.

In complete contrast to before dissolution, all SEM cross-sectional images of samples after dissolution show the disappearance of needle-like crystals protruding above the surface of the compacts. Needles were still present on (and limited to) the surface; however, they were oriented parallel rather than perpendicular to the surface.

Some of the largest needle crystals that were embedded comparatively deep within the compacts were not dissolved or washed away. For example, 2C cross-sectional image on day 28 (also included as a larger image in Figure S4) reveals several outward protruding crystals after the dissolution, with additional smaller crystals that presumably grew during dissolution testing, appearing around and on top of the larger crystals. This order of crystallization is highly likely considering that the storage-induced crystallization yielded outward growing crystals, whereas the solution-mediated crystallization yielded crystals in line with the surface.

Another profound difference is the presence of additional surface morphology not observed prior to dissolution testing. Spherulite structures were visible on the surface of multiple samples in Figure 5. Cross-sectional images of these same regions reveal compact surfaces indentations, tens of micrometers, even up to 100 μm deep, which were covered exclusively by the spherulite-like structures.

3.3.3. Solid-State Transformations Occurring during Dissolution. The heterogeneity of the sample surfaces upon 45 min of dissolution testing is visibly evident from Figure 6. Already at the macroscopic level, distinctive regions characterized by color and texture can be identified. The characterization techniques allowed the targeted characterization of these different regions, as well as the overall solid-state and chemical analysis at the surfaces of the samples. The combination of ATR FTIR (with a sampling diameter of approximately 2 mm) and XRD (with the whole sample under rotation) was especially suitable for this purpose.

Both XRD (Figure 7) and ATR FTIR (Figure 8) results indicate that crystallization also occurred during dissolution. For instance, diffractograms of the uncoated day 0 and day 3 samples after dissolution testing show crystalline peaks above the amorphous halo that were not present prior to dissolution. Crystals formed during storage also dissolved during the

https://dx.doi.org/10.1021/acs.molpharmaceut.9b01263
Mol. Pharmaceutics 2020, 17, 1248−1260

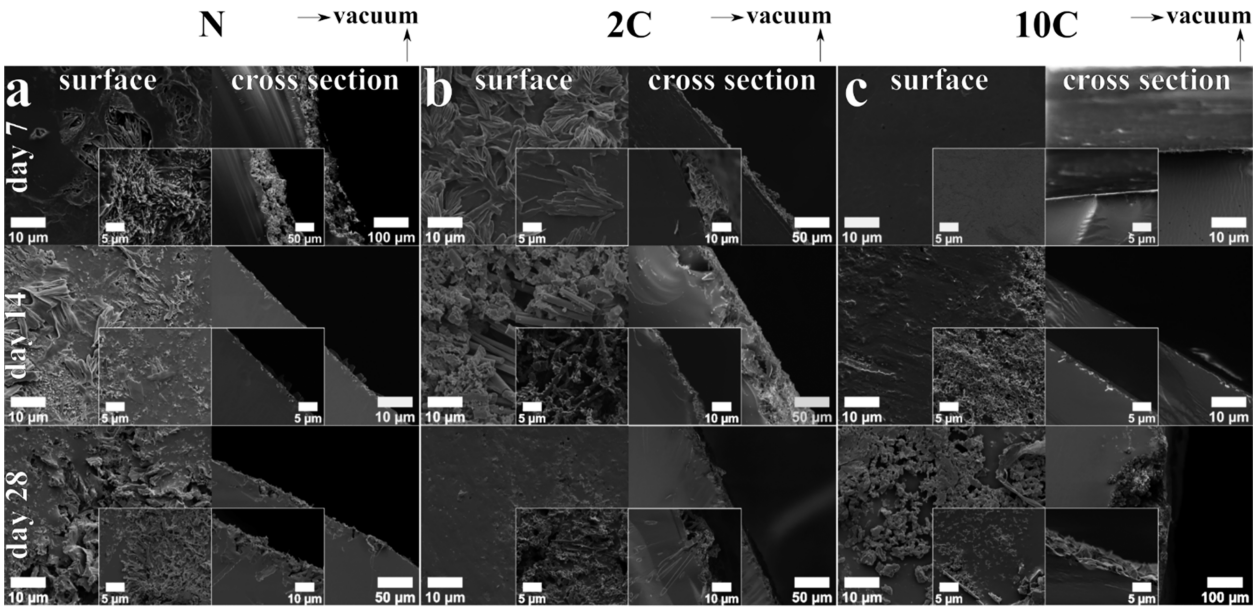

Figure 5. SEM micrographs of the top surface and cross sections of amorphous indomethacin compacts stored at 30 °C/75%RH that underwent intrinsic dissolution testing for 45 min; (a) uncoated (N), (b) PVP-coated with two spraying cycles (2C), and (c) PVP-coated with ten spraying cycles (10C). The black areas on the top right of some cross-sectional images represent a vacuum. This is also indicated by arrows in the figure.

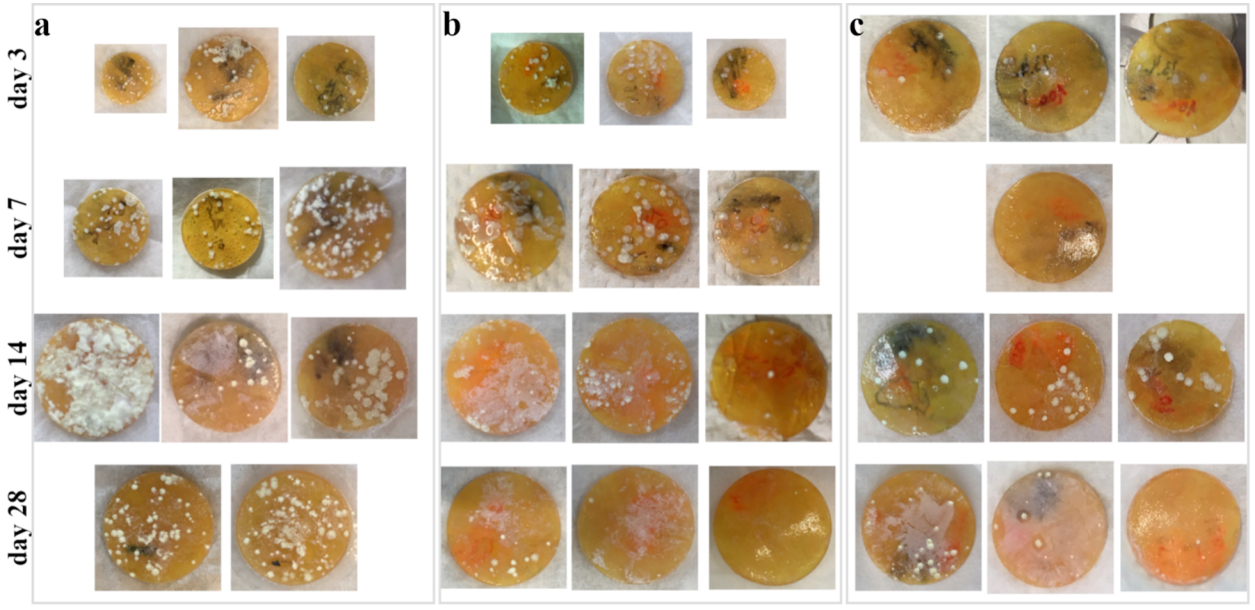

Figure 6. Photographs of compacts after 45 min of dissolution testing: (a) uncoated (N), (b) PVP-coated with two spraying cycles (2C), and (c) PVP-coated with ten spraying cycles (10C). Marker pen writings (in red and black) at the bottom of compacts are visible due to the transparency of the samples.

dissolution study, leading to an apparent decrease in crystallinity. This is evident from Figure 7b, for example, with 2C day 14 and day 28 samples, which were more amorphous after than prior to dissolution.

ATR FTIR spectra provide evidence that the PVP dissolved during dissolution. This conclusion is made based on the complete absence of the PVP signal after dissolution (Figure 8).

Multiple solid-state forms were identified after 45 min of dissolution testing. Crystallization during dissolution, as well as storage, was predominantly to the α form of indomethacin. However, some peaks in the XRD diffractograms also indicate the formation of the ε form, though to a lesser extent than the α form. The presence of the ε form is more evident from the ATR FTIR measurements, in which this polymorph was detected in a significantly larger number of samples, due to the targeted analysis. The formation of the ε form was only observed upon, and never prior to, dissolution.

4. DISCUSSION

4.1. (Pre)Formulation Aspects. The use of vacuum compression (MeltPrep) enabled the preparation of air-bubble-free compacts (tablet cores) without any mechanical grinding. This preparation method preserves the amorphous nature of indomethacin glass and avoids any potential crystallization induced by grinding and compaction, which

https://dx.doi.org/10.1021/acs.molpharmaceut.9b01263
Mol. Pharmaceutics 2020, 17, 1248−1260

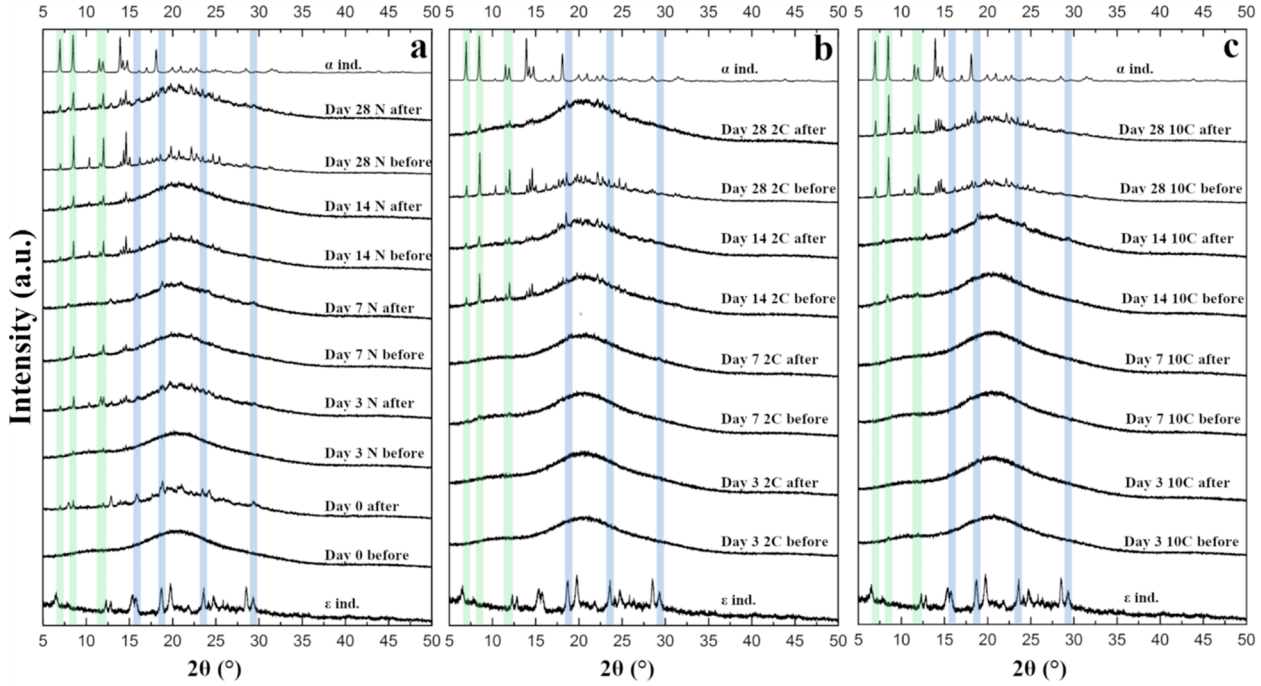

Figure 7. XRD reflection patterns of compacts before and after 45 min of dissolution testing: (a) uncoated (N), (b) PVP-coated with two spraying cycles (2C), and (c) PVP-coated with ten spraying cycles (10C). Characteristic peaks of α and ε forms of indomethacin are marked in green and blue, respectively.

may be present in the case of compressed amorphous powders. Further, vacuum compression minimizes the existence of any voids and free surfaces typically present upon mechanical compression, which would otherwise enable surface-facilitated crystallization within the compacts. One flat face of such tablet cores was then spray-coated with PVP. The approach used in this study was to simplify the "formulation" in order to single-out the impact of a single excipient, in this case, PVP, on storage and dissolution behavior, and thus to exclude the complicating effect of further components on data interpretation, such as any potential film plasticizer. In the design of the storage study, the moisture acted as a coating plasticizer. No drying, peeling, or cracking of the film coating was observed in the time frame of the study by visual inspection. The aqueous coating solution employed was considered more suitable to preserve amorphousness than an organic-based solution, as the latter is more likely to dissolve the drug and thereby induce crystallization partially.[29] The poor aqueous solubility of the drug (indomethacin) thus actually works in favor of aqueous-based coating systems. No change in color or opacity, indicating crystallization after applying the coatings, was observed upon visual inspection. Unlike with compressed amorphous powders, visual inspection of MeltPrep compacts was possible due to the transparency, characteristic for amorphous glasses, being preserved.

It is important to note that the studied coatings, being hundreds of nanometers to a micrometer thick, were much thinner than the tablet-like compacts, at more than a millimeter in thickness. Hence, the polymer coatings are considered to be thin in this context. In comparison, previous studies on storage stability performance of surface coatings have typically employed coatings that are several nm (up to 10−20 nm) thick, on amorphous films that were tens of μm thick.[16] The dissolution performance was assessed with coated amorphous particles, typically 45−100 μm in size.[5,6,13] Overall, the employed sample preparation techniques, vacuum compression molding, and spray coating offered high precision and control and are likely to be suitable for the other drug−polymer systems as well.

It is also important to highlight that our dissolution study involved testing of a whole polymer-coated dosage form (with one polymer-coated surface exposed to medium) rather than individually coated particles dispersed in a dissolution vessel, which limits the interpretation of the results in the present study in relation to these previous studies. Single compact and individual particle motions in the dissolution medium differ significantly. Further, the total amount of polymer is much lower for coated compacts then for coated drug particles.

4.2. Properties of PVP (Films) That Govern Surface Stability during Storage. There are multiple properties of PVP that govern its effect on the amorphous drug behavior during storage and dissolution. In general, the following properties of polymers affect the stabilization efficacy during storage: (i) T_g and the antiplasticizing effect, (ii) presence of specific drug−polymer interactions, (iii) drug−polymer miscibility, (iv) hygroscopicity, and (v) viscosity (related to M_w) of the polymer.[17]

The stabilizing role of PVP during storage is supported by its ability to interact with the drug specifically. Molecularly dispersed PVP in concentrations as low as 1% have been found to reduce amorphous indomethacin crystallization rates during storage at 30 °C (the humidity was not reported).[7] The mechanism of stabilization is not only the antiplasticizing effect (raising the T_g of the drug).[30] Specific hydrogen bonding between the hydroxyl group of indomethacin and carbonyl group of PVP was found to be the main factor preventing the hydrogen bonding within indomethacin dimers, which would lead to crystallization.[24] Another polymer, Eudragit E PO, which is capable of forming ionic bonds with indomethacin,[31] was found to be an even more efficient inhibitor of

https://dx.doi.org/10.1021/acs.molpharmaceut.9b01263
Mol. Pharmaceutics 2020, 17, 1248−1260

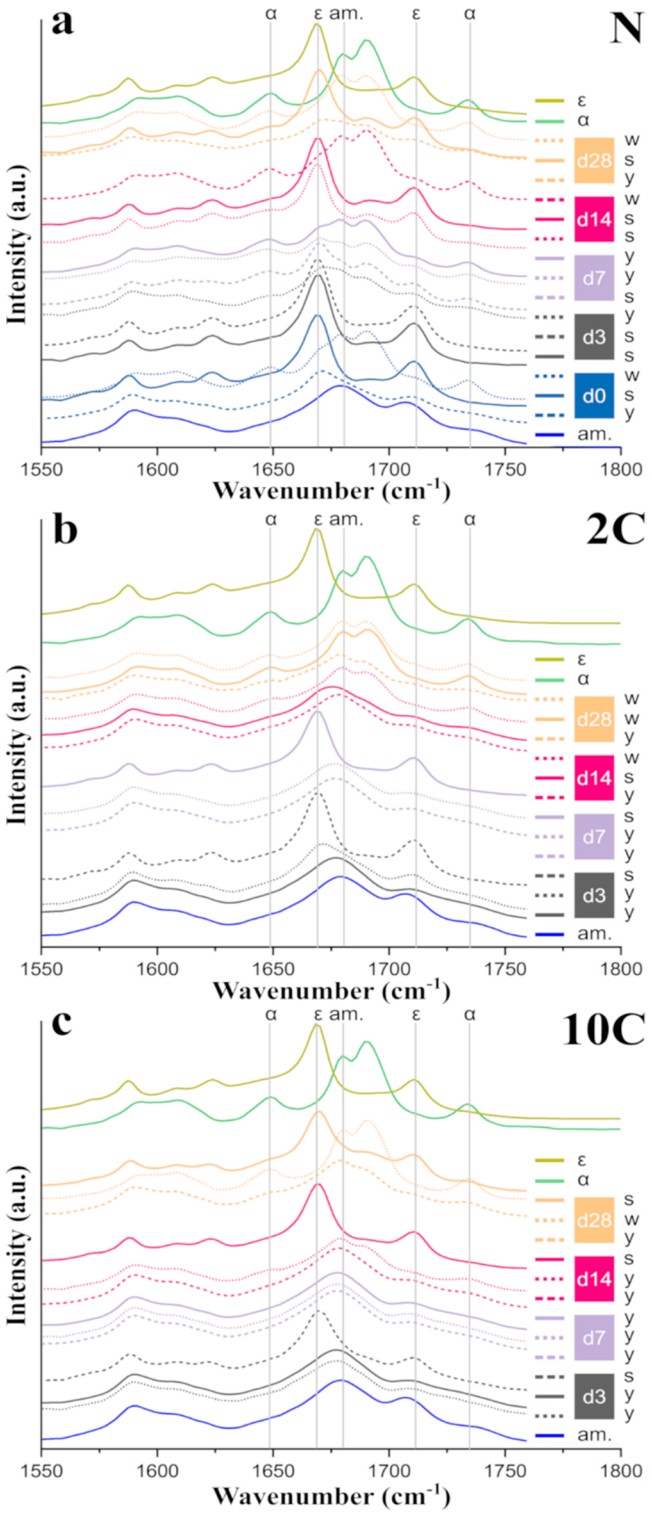

Figure 8. ATR FTIR spectra of compacts after 45 min of dissolution testing: (a) uncoated (N), (b) PVP-coated with two spraying cycles (2C), and (c) PVP-coated with ten spraying cycles (10C). Where applicable, different targeted areas at the surface of compacts (spot (s), yellow (y), and diffuse white regions (w)) are indicated in the legend; am = amorphous.

crystallization, further indicating the importance of molecular interactions.[32] Similar findings have been reported for other drugs as well.[33] Recent reports on effective nanocoating materials have all relied on ionic interactions.[5,6,13] On the other hand, hydrogen bonding or other molecular interactions on their own are an insufficient predictor of stabilization, as the vinylpyrolidone (VP) dimer had little effect as a crystallization inhibitor, in contrast to polymeric PVP.[11] Indeed, even though the extent of hydrogen bonding across different grades of PVP and indomethacin did not differ,[34] grades with higher molecular weight and viscosity were found to be more efficient stabilizers compared to the lower molecular weight and viscosity grades.[34−36] In theory, drug−polymer interactions in the current study would be visible in ATR FTIR spectra of 2C samples (Figure 3b), in which both drug and the polymer peaks were observed. However, these two components had varying signal intensities, which hindered the ability for interaction detection. Although we did not detect hydrogen bonding with ATR FTIR in this study (mainly due to the interactions being limited to the drug−polymer interface, and the sampling volume of ATR FTIR being much larger), such interactions at the very thin drug−polymer interfacial layer are probable, since they have been reported for indomethacin-PVP solid dispersions. In addition, hydrogen bonding of indomethacin or PVP with water molecules could have masked any detectable carbonyl peak shifts arising from drug−polymer interactions. The observed shift of PVP carbonyl peak at around 1650 cm^{-1} toward lower wavenumbers in the 10C-coated samples (Figure 3c) indicates PVP−water interactions. Wan et al.[37] reported this red shift in ATR FTIR spectra of PVP K90 films exposed to 70% RH at 25 °C.

Another related and important factor in relation to storage solid-state stability, particularly upon exposure to high humidity conditions, is polymer hygroscopicity.[17] Our ATR FTIR spectra of 10C coatings show a PVP carbonyl peak shift to lower wavenumbers during storage, which is evidence for PVP−water interactions. In this respect, PVP is highly hygroscopic, as it absorbs approximately 40% moisture upon exposure to 80% RH,[38] or 38% at the humidity used in this study (75% RH).[17] Some studies suggest that hygroscopic polymers such as PVP may prefer to hydrogen bond with water instead of the drug,[17,39] which could make them less effective stabilizers compared to nonhygroscopic polymers (such as Soluplus or Eudragit E PO, for example).[17] Out of the latter two, the less hygroscopic similar grade of Eudragit E was found more effective at amorphous form stabilization during storage than Soluplus, which supports this view.[40] In the current study, despite their hygroscopicity, PVP coatings stabilized the amorphous drug during storage, and their effect depended on the coating thickness. This could potentially be caused by the greater barrier provided by a thicker coating, making the outward growth of needles more challenging.

During storage, we observed axial (outward) crystal growth at the surface of pure amorphous indomethacin compacts and compacts spray-coated with PVP. Lateral crystal growth (sideways, with respect to the sample surface in between two microscope coverslips) of amorphous nifedipine[11] and indomethacin[41] has been reported earlier. The authors argued that the most likely mechanism for this phenomenon is the surface transport of molecules originating from the glass surface. In support of this explanation, we and the others[4,10] have observed depletion zones, which look like microcracks in between amorphous and crystalline areas at the surface, as shown in Figure S2.

The crystallization during storage mainly yielded the *α* form of indomethacin. This is in agreement with previous studies of amorphous indomethacin crystallization at high humidity.[26,27]

https://dx.doi.org/10.1021/acs.molpharmaceut.9b01263
Mol. Pharmaceutics 2020, 17, 1248−1260

4.3. Dissolution Performance. According to the Noyes–Whitney equation, factors influencing dissolution rate include (i) the solubility of the solid at the dissolving surface, which is dependent on the solid-state form of the solid (amorphous versus existing or different crystalline forms forming during dissolution) and presence of any solubility enhancers such as polymers, (ii) dissolving surface area, which can be affected by potential crystallization occurring during dissolution, as well as on the morphology and surface coverage with newly formed crystals, and (iii) thickness of the diffusion layer, which is affected by the viscosity at the surface.

In addition to the factors governing the effect of PVP on stability during storage, during dissolution, the presence of a (pre)dissolved polymer can inhibit crystallization based on the following mechanisms: (i) cosolvent effect of the polymer that reduces the supersaturation and, thus, the driving force for recrystallization, (ii) coverage of growing crystal faces with the polymer, and (iii) presence of polymer film at the surface, which hinders nucleation.[42]

Even though beneficial to the stability of the amorphous forms, the higher viscosity afforded by the polymer might adversely affect dissolution. It is expected that the presence of PVP in the dissolution medium provides a parachute effect for maintaining the supersaturation of indomethacin.[43] The incorporation method can also have an effect, and solid dispersions were shown to be better at maintaining supersaturation than the predissolved polymer[42] or drug and polymer physical mixtures. In the current study, PVP-coated samples stored at high humidity did not outperform the IDR of fresh amorphous indomethacin; however, the physical stabilization during storage and maintenance of early-stage IDR were achieved. The increase in viscosity caused by the PVP, which has an average molecular weight of 40 000, is probably one of the reasons for the observed dissolution behavior. The impaired performance in the latter stages of dissolution was especially evident for the 10C-coated samples. Such an effect has previously been reported with indomethacin spray-dried with PVP: a decreased IDR with increased PVP content was attributed to increasing the viscosity of the particle-localized PVP.[44] Small increases in medium viscosity, representing those of water (0.7 mPa s), milk (1.4 mPa s), or a nutrient drink (12.3 mPa s), have also been shown to significantly lower the dissolution rate.[45] In our case, the overall amount of PVP dissolved in the medium is small and estimated to be approximately 0.005 mg/mL for 10C-coated samples.

During the initial (early-stage) dissolution period, we can assume that no solution-mediated crystallization is taking place (no change in the surface area nor recrystallization-induced change in solubility), and the polymer is not fully dissolved yet (viscosity effects may be present). In this stage, there were no differences in the IDR of freshly prepared uncoated amorphous indomethacin and short-term stored coated samples (2C and 10C), in contrast to all stored uncoated (N) samples and long-term stored coated samples (2C and 10C), that had decreased IDRs. This would indicate that the dissolution performance in this stage is mainly dependent on the storage time, or in other words, the level of crystallinity present prior to dissolution. As the crystallinity is increasing during storage, the solubility at the surface is decreasing (as well as the dissolution rate). As an opposing factor, the storage-induced formation of α indomethacin needles protruding above the surface increases the surface area (and dissolution rate), although this effect is more significant for the uncoated samples, in which the needles formed sooner and to a greater extent. The observed behavior indicates that the polymer coatings are not having a significant effect on this early stage of dissolution, with the effects of increased viscosity at the surface (decreasing the dissolution rate) on the one hand, and increased solubility of the drug (and the dissolution rate) on the other hand, canceling each other out.

During the later stages of dissolution, once presumably solution-mediated recrystallization has already started (as indicated by the curvature in dissolution profiles), the factors influencing the rate of dissolution are changed. Most importantly, the recrystallization from the solution causes a decrease in solubility (and dissolution rate) and an increase in the dissolving surface area (and dissolution rate). Further, at this stage, the polymer has already largely dissolved but is likely to be still affecting the surface crystallization. Based on the appearance of samples collected after dissolution, the presence of polymer has a surface-smoothing effect by virtue of crystallization inhibition, which overall decreases the dissolution rate, by lowering the surface area despite maintaining the amorphous solubility (in comparison to uncoated samples). Further, the increased viscosity and/or higher PVP concentration available for interaction at this stage may hinder the release. Higher concentrations of PVP can cover the dissolving surface to a greater extent, which hinders nucleation and prevents the growth of existing crystal faces. Together, these factors can explain why the thicker PVP coating inhibits the dissolution more strongly in this stage, and the performance of samples introducing larger amounts of PVP is worse than that of the α indomethacin and thinner coated samples.

In addition to variability caused by the dynamic nature of competing dissolution and recrystallization processes, specific test conditions such as the actual agitation speed and behavior of submerged compacts may have contributed to the variability in the dissolution profiles. Namely, in addition to the dissolution-profile curvature indicating solution-mediated solid-state transformation, sigmoidal curvature was also observed in some of the dissolution profiles. This could, at least partly, be due to the hydrodynamic conditions in the vessel. Namely, as opposed to the rotating disk apparatus, where the studied surface is fixed and exposed to the same hydrodynamic conditions throughout the test, in the current approach, the tablet in the vessel might end up with either the studied (uncoated or PVP-coated) or nail polish side facing upward in the medium. In addition, many of the compacts were mostly static (lacking movement) at the beginning of the tests and started substantially more movement after approximately 10 min.

In addition to the formation of the α polymorph, which was also detected during storage, crystallization to the ε form also occurred during dissolution in phosphate buffer at pH 6.8. This is consistent with our previous studies[18,46] and an unnamed polymorph of indomethacin reported by others.[47,48]

The increase in surface area during dissolution occurred mainly due to the formation of ε form-rich spherulite-like structures that formed indentations tens of micrometers deep into the surface. The porosity of these spherulite structures likely facilitated further dissolution and solution-mediated crystallization (relative to their size and number on each of the tested samples), in addition to the increase in the surface area caused by the formation of α indomethacin needles.

https://dx.doi.org/10.1021/acs.molpharmaceut.9b01263
Mol. Pharmaceutics 2020, 17, 1248–1260

The selected analysis methods were complementary and allowed a better understanding of crystal habit, localization, and solid-state form, particularly after dissolution. The macroscopically visible size of the white spots and diffuse white areas that formed during dissolution testing (Figure 6) enabled their targeted analysis with SEM and ATR FTIR. With SEM, white spots were characterized by spherulite-like structures that formed surface indentations. When these regions were probed with ATR FTIR, they showed spectra, corresponding to the ε form of indomethacin. Similarly, diffuse white areas were characterized by needle morphology with SEM and ATR FTIR spectra corresponding to α indomethacin.

5. CONCLUSIONS

This study shows that while crystallization inhibition during storage is important, the other factors associated with the polymers and the coatings themselves can have an equally important effect on dissolution. The surface stabilization of amorphous drug during storage, as well as its dissolution performance in each of the stability test points, were investigated using a simple tablet-like dosage form spray-coated as a whole with a thin polymer layer. The selected characterization techniques (SEM, ATR FTIR, and XRD) provided complementary data that aided the interpretation of intrinsic dissolution results.

This study showed that thin polymer coatings are capable of delaying the onset of crystallization of amorphous drug compacts stored at an elevated humidity. Thicker, micrometer range coatings provided two times longer stabilization than the thinner coatings, which were hundreds of nanometers thick.

The improved storage stabilization of the amorphous drugs can, at least to some extent, maintain their IDR, but this does not necessarily guarantee an improvement of the IDRs. Besides surface stability, other factors (such as the surface, the extent of precipitation, and the coatings themselves) contribute to the complexity of dissolution phenomena, and the overall dissolution performance reflects the interplay of all of these contributing factors.

This study focused, from a pharmaceutical perspective, on amorphous surface phenomena, mimicking as much as possible the standards that would be used by the pharmaceutical industry and regulators, such as tablet-like compacts, a broadly used pharmaceutical excipient, and spray coating as well as pharmacopoeial dissolution tests. This research brings us a step closer to understanding and utilizing surface crystallization and its inhibition in amorphous drug formulations.

■ ASSOCIATED CONTENT

Supporting Information

The Supporting Information is available free of charge at https://pubs.acs.org/doi/10.1021/acs.molpharmaceut.9b01263.

SEM images of day 0 uncoated sample; SEM surface images of day 3 uncoated samples upon storage; XRD penetration depth versus incidence angle profiles; SEM cross-sectional image of 2C coated sample upon storage for 28 days and consequent dissolution for 45 min (PDF)

■ AUTHOR INFORMATION

Corresponding Author

Dunja Novakovic − *Drug Research Program, Division of Pharmaceutical Chemistry and Technology, Faculty of Pharmacy, University of Helsinki, 00014 Helsinki, Finland;* orcid.org/0000-0003-2058-2194; Email: dunja.novakovic@helsinki.fi

Authors

Leena Peltonen − *Drug Research Program, Division of Pharmaceutical Chemistry and Technology, Faculty of Pharmacy, University of Helsinki, 00014 Helsinki, Finland*

Antti Isomäki − *Biomedicum Imaging Unit, Faculty of Medicine, University of Helsinki, 00014 Helsinki, Finland*

Sara J. Fraser-Miller − *Dodd-Walls Center for Photonic and Quantum Technologies, Department of Chemistry, University of Otago, 9016 Dunedin, New Zealand*

Line Hagner Nielsen − *Department of Health Technology, Technical University of Denmark, 2800 Kgs Lyngby, Denmark;* orcid.org/0000-0002-3789-4816

Timo Laaksonen − *Laboratory of Chemistry and Bioengineering, Tampere University of Technology, 33720 Tampere, Finland*

Clare J. Strachan − *Drug Research Program, Division of Pharmaceutical Chemistry and Technology, Faculty of Pharmacy, University of Helsinki, 00014 Helsinki, Finland;* orcid.org/0000-0003-3134-8918

Complete contact information is available at: https://pubs.acs.org/10.1021/acs.molpharmaceut.9b01263

Author Contributions

The manuscript was written through the contributions of all authors. All authors have given approval to the final version of the manuscript.

Funding

NordForsk for the Nordic University Hub project no. 85352 (Nordic POP, Patient Oriented Products) is gratefully acknowledged for providing financial support in the form of the mobility project grant for D.N. D.N. also gratefully acknowledges the Doctoral Program in Drug Research funding provided by the University of Helsinki. C.S. acknowledges the Academy of Finland (grant no. 289398).

Notes

The authors declare no competing financial interest.

■ ACKNOWLEDGMENTS

Sanna Sistonen and Heikki Räikkönen from the University of Helsinki are gratefully acknowledged for their help with some of the dissolution and XRD measurements, respectively. Heikki Suhonen from the University of Helsinki is acknowledged for the XRD penetration depth calculations. The Electron Microscopy Unit at the University of Helsinki is acknowledged for providing access to the SEM facilities and technical support. Members of the IDUN laboratories at the Technical University of Denmark (DTU Health Tech) and the Department of Pharmacy at the University of Copenhagen are acknowledged for providing a constructive atmosphere during DN's research visit to Copenhagen. In particular, Jacob Bannow, Chiara Mazzoni, and Juliane Fjelrad Christfort are thanked for their help and training in using MeltPrep and spray coating instruments, respectively.

■ ABBREVIATIONS

N, uncoated; 2C, coated with two spraying cycles; 10C, coated with ten spraying cycles; PVP, polyvinylpyrolidone; SEM, scanning electron microscopy; XRD, X-ray diffraction; ATR, FTIR attenuated total reflectance Fourier transform infrared spectroscopy; IDR, intrinsic dissolution rate

■ REFERENCES

(1) Wu, T.; Yu, L. Surface crystallization of indomethacin below T_g. *Pharm. Res.* **2006**, *23* (10), 2350−2355.

(2) Zhu, L.; Jona, J.; Nagapudi, K.; Wu, T. Fast surface crystallization of amorphous griseofulvin below T_g. *Pharm. Res.* **2010**, *27* (8), 1558−1567.

(3) Zhu, L.; Wong, L.; Yu, L. Surface-enhanced crystallization of amorphous nifedipine. *Mol. Pharmaceutics* **2008**, *5* (6), 921−926.

(4) Shi, Q.; Cai, T. Fast crystal growth of amorphous griseofulvin: Relations between bulk and surface growth modes. *Cryst. Growth Des.* **2016**, *16* (6), 3279−3286.

(5) Zeng, A.; Yao, X.; Gui, Y.; Li, Y.; Jones, K. J.; Yu, L. Inhibiting surface crystallization and improving dissolution of amorphous loratadine by dextran sulfate nanocoating. *J. Pharm. Sci.* **2019**, *108* (7), 2391−2396.

(6) Gui, Y.; Chen, Y.; Chen, Z.; Jones, K. J.; Yu, L. Improving stability and dissolution of amorphous clofazimine by polymer nanocoating. *Pharm. Res.* **2019**, *36* (5), 67.

(7) Crowley, K. J.; Zografi, G. The effect of low concentrations of molecularly dispersed poly(vinylpyrrolidone) on indomethacin crystallization from the amorphous state. *Pharm. Res.* **2003**, *20* (9), 1417−1422.

(8) Zhu, L.; Brian, C. W.; Swallen, S. F.; Straus, P. T.; Ediger, M. D.; Yu, L. Surface self-diffusion of an organic glass. *Phys. Rev. Lett.* **2011**, *106* (25), 256103.

(9) Huang, C.; Ruan, S.; Cai, T.; Yu, L. Fast surface diffusion and crystallization of amorphous griseofulvin. *J. Phys. Chem. B* **2017**, *121* (40), 9463−9468.

(10) Hasebe, M.; Musumeci, D.; Yu, L. Fast surface crystallization of molecular glasses: Creation of depletion zones by surface diffusion and crystallization flux. *J. Phys. Chem. B* **2015**, *119* (7), 3304−3311.

(11) Cai, T.; Zhu, L.; Yu, L. Crystallization of organic glasses: Effects of polymer additives on bulk and surface crystal growth in amorphous nifedipine. *Pharm. Res.* **2011**, *28* (10), 2458−2466.

(12) Wu, T.; Sun, Y.; Li, N.; de Villiers, M. M.; Yu, L. Inhibiting surface crystallization of amorphous indomethacin by nanocoating. *Langmuir* **2007**, *23* (9), 5148−5153.

(13) Li, Y.; Yu, J.; Hu, S.; Chen, Z.; Sacchetti, M.; Sun, C. C.; Yu, L. Polymer nanocoating of amorphous drugs for improving stability, dissolution, powder flow, and tabletability: The case of chitosan-coated indomethacin. *Mol. Pharmaceutics* **2019**, *16* (3), 1305−1311.

(14) Hsu, H.-Y.; Harris, M. T.; Toth, S.; Simpson, G. J. Drop printing of pharmaceuticals: Effect of molecular weight on PEG coated-naproxen/PEG 3350 solid dispersions. *AIChE J.* **2015**, *61* (12), 4502−4508.

(15) Capece, M.; Davé, R. Enhanced physical stability of amorphous drug formulations via dry polymer coating. *J. Pharm. Sci.* **2015**, *104* (6), 2076−2084.

(16) Teerakapibal, R.; Gui, Y.; Yu, L. Gelatin nano-coating for inhibiting surface crystallization of amorphous drugs. *Pharm. Res.* **2018**, *35* (1), 23.

(17) Ng, Y. C.; Yang, Z.; McAuley, W. J.; Qi, S. Stabilisation of amorphous drugs under high humidity using pharmaceutical thin films. *Eur. J. Pharm. Biopharm.* **2013**, *84* (3), 555−565.

(18) Surwase, S. A.; Boetker, J. P.; Saville, D.; Boyd, B. J.; Gordon, K. C.; Peltonen, L.; Strachan, C. J. Indomethacin: New polymorphs of an old drug. *Mol. Pharmaceutics* **2013**, *10* (12), 4472−4480.

(19) Koranne, S.; Thakral, S.; Suryanarayanan, R. Effect of formulation and process parameters on the disproportionation of indomethacin sodium in buffered lyophilized formulations. *Pharm. Res.* **2018**, *35* (1), 1.

(20) Treffer, D.; Troiss, A.; Khinast, J. A novel tool to standardize rheology testing of molten polymers for pharmaceutical applications. *Int. J. Pharm.* **2015**, *495* (1), 474−481.

(21) Eder, S.; Beretta, M.; Witschnigg, A.; Koutsamanis, I.; Eggenreich, K.; Khinast, J. G.; Koscher, G.; Paudel, A.; Nickisch, K.; Friedrich, M.; Froehlich, E.; Roblegg, E. Establishment of a molding procedure to facilitate formulation development for co-extrudates. *AAPS PharmSciTech* **2017**, *18* (8), 2971−2976.

(22) Bose, S.; Keller, S. S.; Alstrøm, T. S.; Boisen, A.; Almdal, K. Process optimization of ultrasonic spray coating of polymer films. *Langmuir* **2013**, *29* (23), 6911−6919.

(23) Imaizumi, H.; Nambu, N.; Nagai, T. Stabilization of amorphous state of indomethacin by solid dispersion in polyvinylpolypyrrolidone. *Chem. Pharm. Bull.* **1983**, *31* (7), 2510−2512.

(24) Taylor, L. S.; Zografi, G. Spectroscopic characterization of interactions between PVP and indomethacin in amorphous molecular dispersions. *Pharm. Res.* **1997**, *14* (12), 1691−1698.

(25) Buckton, G.; Ambarkhane, A.; Pincott, K. The use of inverse phase gas chromatography to study the glass transition temperature of a powder surface. *Pharm. Res.* **2004**, *21* (9), 1554−1557.

(26) Andronis, V.; Yoshioka, M.; Zografi, G. Effects of sorbed water on the crystallization of indomethacin from the amorphous state. *J. Pharm. Sci.* **1997**, *86* (3), 346−351.

(27) Novakovic, D.; Saarinen, J.; Rojalin, T.; Antikainen, O.; Fraser-Miller, S. J.; Laaksonen, T.; Peltonen, L.; Isomäki, A.; Strachan, C. J. Multimodal nonlinear optical imaging for sensitive detection of multiple pharmaceutical solid-state forms and surface transformations. *Anal. Chem.* **2017**, *89* (21), 11460−11467.

(28) Bahl, D.; Bogner, R. H. Amorphization alone does not account for the enhancement of solubility of drug co-ground with silicate: The case of indomethacin. *AAPS PharmSciTech* **2008**, *9* (1), 146−153.

(29) Sun, Y.; Zhu, L.; Wu, T.; Cai, T.; Gunn, E. M.; Yu, L. Stability of amorphous pharmaceutical solids: Crystal growth mechanisms and effect of polymer additives. *AAPS J.* **2012**, *14* (3), 380−388.

(30) Yoshioka, M.; Hancock, B. C.; Zografi, G. Inhibition of indomethacin crystallization in poly(vinylpyrrolidone) coprecipitates. *J. Pharm. Sci.* **1995**, *84* (8), 983−986.

(31) Liu, H.; Zhang, X.; Suwardie, H.; Wang, P.; Gogos, C. G. Miscibility studies of indomethacin and Eudragit® E PO by thermal, rheological, and spectroscopic analysis. *J. Pharm. Sci.* **2012**, *101* (6), 2204−2212.

(32) Chokshi, R. J.; Shah, N. H.; Sandhu, H. K.; Malick, A. W.; Zia, H. Stabilization of low glass transition temperature indomethacin formulations: Impact of polymer-type and its concentration. *J. Pharm. Sci.* **2008**, *97* (6), 2286−2298.

(33) Mistry, P.; Mohapatra, S.; Gopinath, T.; Vogt, F. G.; Suryanarayanan, R. Role of the strength of drug−polymer interactions on the molecular mobility and crystallization inhibition in ketoconazole solid dispersions. *Mol. Pharmaceutics* **2015**, *12* (9), 3339−3350.

(34) Mohapatra, S.; Samanta, S.; Kothari, K.; Mistry, P.; Suryanarayanan, R. Effect of polymer molecular weight on the crystallization behavior of indomethacin amorphous solid dispersions. *Cryst. Growth Des.* **2017**, *17* (6), 3142−3150.

(35) Kestur, U. S.; Lee, H.; Santiago, D.; Rinaldi, C.; Won, Y.-Y.; Taylor, L. S. Effects of the molecular weight and concentration of polymer additives, and temperature on the melt crystallization kinetics of a small drug molecule. *Cryst. Growth Des.* **2010**, *10* (8), 3585−3595.

(36) Huang, C.; Powell, C. T.; Sun, Y.; Cai, T.; Yu, L. Effect of low-concentration polymers on crystal growth in molecular glasses: A controlling role for polymer segmental mobility relative to host dynamics. *J. Phys. Chem. B* **2017**, *121* (8), 1963−1971.

(37) Wan, L.-S.; Huang, X.-J.; Xu, Z.-K. Diffusion and structure of water in polymers containing N-vinyl-2-pyrrolidone. *J. Phys. Chem. B* **2007**, *111* (5), 922−928.

(38) Fitzpatrick, S.; McCabe, J. F.; Petts, C. R.; Booth, S. W. Effect of moisture on polyvinylpyrrolidone in accelerated stability testing. *Int. J. Pharm.* **2002**, *246* (1), 143−151.

https://dx.doi.org/10.1021/acs.molpharmaceut.9b01263
Mol. Pharmaceutics 2020, 17, 1248−1260

(39) Rumondor, A. C. F.; Taylor, L. S. Effect of polymer hygroscopicity on the phase behavior of amorphous solid dispersions in the presence of moisture. *Mol. Pharmaceutics* **2010**, *7* (2), 477−490.
(40) Priemel, P. A.; Laitinen, R.; Barthold, S.; Grohganz, H.; Lehto, V.-P.; Rades, T.; Strachan, C. J. Inhibition of surface crystallisation of amorphous indomethacin particles in physical drug−polymer mixtures. *Int. J. Pharm.* **2013**, *456* (2), 301−306.
(41) Sun, Y.; Zhu, L.; Kearns, K. L.; Ediger, M. D.; Yu, L. Glasses crystallize rapidly at free surfaces by growing crystals upward. *Proc. Natl. Acad. Sci. U. S. A.* **2011**, *108* (15), 5990−5995.
(42) Surwase, S. A.; Itkonen, L.; Aaltonen, J.; Saville, D.; Rades, T.; Peltonen, L.; Strachan, C. J. Polymer incorporation method affects the physical stability of amorphous indomethacin in aqueous suspension. *Eur. J. Pharm. Biopharm.* **2015**, *96*, 32−43.
(43) Alonzo, D. E.; Zhang, G. G. Z.; Zhou, D.; Gao, Y.; Taylor, L. S. Understanding the behavior of amorphous pharmaceutical systems during dissolution. *Pharm. Res.* **2010**, *27* (4), 608−618.
(44) Li, Y.; Rantanen, J.; Yang, M.; Bohr, A. Molecular structure and impact of amorphization strategies on intrinsic dissolution of spray dried indomethacin. *Eur. J. Pharm. Sci.* **2019**, *129*, 1−9.
(45) D'Arcy, D. M.; Persoons, T. Understanding the potential for dissolution simulation to explore the effects of medium viscosity on particulate dissolution. *AAPS PharmSciTech* **2019**, *20* (2), 47.
(46) Novakovic, D.; Isomäki, A.; Pleunis, B.; Fraser-Miller, S. J.; Peltonen, L.; Laaksonen, T.; Strachan, C. J. Understanding dissolution and crystallization with imaging: A surface point of view. *Mol. Pharmaceutics* **2018**, *15* (11), 5361−5373.
(47) Greco, K.; Bogner, R. Crystallization of amorphous indomethacin during dissolution: Effect of processing and annealing. *Mol. Pharmaceutics* **2010**, *7* (5), 1406−1418.
(48) Tres, F.; Treacher, K.; Booth, J.; Hughes, L. P.; Wren, S. A. C.; Aylott, J. W.; Burley, J. C. Indomethacin-Kollidon VA64 extrudates: A mechanistic study of pH-dependent controlled release. *Mol. Pharmaceutics* **2016**, *13* (3), 1166−1175.

https://dx.doi.org/10.1021/acs.molpharmaceut.9b01263
Mol. Pharmaceutics 2020, 17, 1248−1260